Stress tensor: A quantitative indicator of effective volume and stability of helium in metals

Stress tensor: A quantitative indicator of effective volume and stability of helium in metals

H.-B. Zhou[1], S. Jin[1], X.-L. Shu[1], Y. Zhang[1], G.-H. Lu[1(a)] and F. Liu[2]

[1] *Department of Physics, Beihang University - Beijing 100191, China*
[2] *Department of Materials Science and Engineering, University of Utah - Salt Lake City, UT 84112, USA*

Abstract – We demonstrate a quantitative stress indicator as well as a qualitative hard-sphere lattice model to characterize the effective volume and stability of interstitial helium in fcc and bcc metals, based on extensive first-principles total-energy and lattice stress calculations in combination with continuum elastic theory analyses. The concept of stress indicator is believed to be generally applicable to quantify the relative stability of other inert gas elements in metals.

Helium (He) is a typical impurity in metals. The solubility of He in metals is extremely low, yet it can lead to significant changes in microstructure and mechanical properties. The well-known example is the high-temperature He embrittlement at extremely low concentration [1–3]. Helium is produced from (n, α) transmutation reactions in both fission and fusion, resulting in radiation damage and mechanical property degradation of metals [3,4]. Since He has a closed shell electronic structure forming very weak chemical bonding with the host metal atoms, the stability of He in metals should be well characterized by its "effective volume", which is determined by its atomic size relative to the available volume provided by the given interstitial site. For this reason, the relative stability of He at different interstitial sites in a lattice is usually gauged by a lattice model [5–7]. However, this has often caused confusion and controversy [5–7] because the size of an interstitial site can be ambiguous depending on what lattice models are used. Therefore, developing a theoretical model to quantify the He effective volume in metals is fundamental to the understanding of its stability and effects on mechanical properties of metals.

Conventionally, the volume of He at an octahedral interstitial site (OIS) is considered to be larger than that at a tetrahedral interstitial site (TIS) in both face-centered cubic (fcc) and body-centered cubic (bcc) metals [5–7]. This would suggest that He prefer to occupy the OIS instead of TIS. However, the OIS occupation for He is found in fcc metals [8,9], while the TIS occupation is found in bcc metals [5–7,10,11]. The unexpected TIS occupation of He in bcc metals motivated a series of investigations. Seletskaia *et al.* attributed the TIS preference of He in bcc Fe to the magnetism [5], but was contradicted by the first-principles calculations by Zu *et al.* [7]. It was also suggested that a strong hybridization between the He p states and transition metal d states may change the He site preference in bcc metals [5–7]. However, such strong hybridization was questioned by Fu and Willaime [10], given the closed shell structure of He.

The controversy on the site preference of interstitial He in metals stems largely from the lack of a reliable approach to define the effective volume of He, namely the "size" of the TIS *vs.* the OIS; the empirical lattice models used previously [5–7] are incorrect. Here, we develop a unified approach to quantify the effective volume of interstitial He in different metals by the "lattice stress" induced by He, which can be directly calculated using the first-principles methods. We show that the effective volume of He and hence its solution energy scales quadratically with the square of the He-induced stress, following the linear elastic theory, as confirmed by first-principles total-energy and stress calculations of He in ten fcc and bcc metals. Furthermore, we show that the hard-sphere lattice model gives the best empirical estimate of the effective volume of He in both fcc and bcc metals, while the point-lattice and Voronoi polygon model are qualitatively incorrect.

(a)E-mail: LGH@buaa.edu.cn

Table 1: Solution energy (in eV) and formation volume (in Å^3) of He, the He-induced stress (in GPa), the relative stability, and the ratio of stress at the TIS over OIS in fcc and bcc metals.

			fcc					bcc				
			Pd	Al	Au	Pt	Ag	W	Mo	Fe	Cr	V
Solution		TIS	3.82	3.43	3.28	5.18	3.07	6.13	5.21	4.56	5.18	3.05
energy		OIS	3.68	3.25	2.92	4.73	2.82	6.37	5.41	4.77	5.38	3.28
Formation		TIS	9.39	16.2	16.9	10.8	14.7	5.32	5.58	7.85	5.55	5.61
volume		OIS	8.25	13.9	14.8	9.52	12.5	5.56	5.64	8.57	5.72	6.11
σ	TIS	XX						-1.97	-1.79	-2.54	-2.29	-1.31
		YY	-3.33	-2.21	-4.03	-5.24	-2.49	-1.87	-1.76	-2.61	-2.59	-1.79
		ZZ						-1.97	-1.79	-2.54	-2.29	-1.31
	OIS	XX						-1.58	-1.48	-2.38	-1.98	-1.59
		YY	-2.82	-1.89	-3.42	-4.51	-2.05	-1.58	-1.48	-2.38	-1.98	-1.59
		ZZ						-2.89	-2.55	-3.24	-3.44	-1.81
$E_s^{\mathrm{TIS}}/E_s^{\mathrm{OIS}}$			1.04	1.06	1.12	1.10	1.09	0.96	0.96	0.96	0.96	0.93
$\sum \sigma_{ii,\mathrm{TIS}}^2 / \sum \sigma_{ii,\mathrm{OIS}}^2$			1.39	1.37	1.39	1.35	1.48	0.84	0.87	0.90	0.87	0.80

Our total energy calculations were performed within the density functional theory as implemented in the VASP code [12,13]. We use the generalized gradient approximation of Perdew and Wang [14] and projected augmented wave potentials [15]. We found that a plane wave energy cutoff of 350 eV is large enough for all metal systems to ensure the total energy and stress convergence, consistent with previous calculations [6,11,16–20]. The Brillouin zone sampling was performed using the Monkhorst-Pack scheme [21], with $6 \times 6 \times 6$ k-point meshes for a 32 atom supercell in fcc metals and $5 \times 5 \times 5$ k-point meshes for a 54 atom supercell in bcc metals. The energy minimization was converged until the forces on all the atoms are less than 10^{-3} eV Å^{-1}. We check the supercell size by investigating the solution energy and the stress for the supercell containing different number of atoms. The solution energy of He converges at the 54-atom supercell in comparison with the 128-atom one. For example, the solution energy of He at the TIS in W is 6.13 eV for the 54-atom supercell, while it is 6.14 eV for the 128-atom supercell. Further, it is shown that the stress induced by He in a 128-atom cell equals to that in the 54-atom cell scaled by their volume ratio.

A metal lattice is stress free at equilibrium. When a He atom is introduced at an interstitial site, it induces a lattice stress depending on He density. In general, this stress has contributions from both the atomic size effect, *i.e.*, the mismatch between the size of He atom and the available volume provided by the interstitial site, and the electronic effect, *i.e.*, the He-induced change of lattice electronic structure giving rise to a quantum stress effect [22]. Then, the He solution energy (E_s) can be well characterized by the He-induced lattice deformation energy, which scales quadratically with the He-induced lattice stress (σ) as $E_s \sim \sum \sigma_{ii}^2/\mathrm{E}$ [23], where double

indices (ii) indicates summation over three Cartesian components, and E is the elastic modulus of the He-doped lattice. Then, we can assess the relative stability of He at different interstitial sites, *i.e.* TIS *vs.* OIS, in a given lattice by the ratio of the He-induced lattice stress at the two sites

$$\frac{E_s^{\mathrm{TIS}}}{E_s^{\mathrm{OIS}}} = \alpha \cdot \frac{\sum \sigma_{ii,\mathrm{TIS}}^2}{\sum \sigma_{ii,\mathrm{OIS}}^2} \tag{1}$$

where the coefficient α is a constant depending on lattice type. To test the above hypothesis, we performed extensive first-principles calculations of interstitial He in ten different metals, including fcc metals of Pd, Al, Au, Pt, and Ag and bcc metals of W, Mo, Fe, Cr, and V. Table 1 shows the calculated He solution energies along with the He-induced lattice stress. Our results of solution energies are in good agreement with previous calculations [5–11]. The main energetic results are the He favors the OIS in fcc metals; while it favors the TIS in bcc metals. The stress results are new and interesting. In all cases the He induces a compressive (negative sign) stress, indicating that the size of He is larger than the available lattice volume. The stress is isotropic in fcc metals because of the symmetric geometry of TIS and OIS structure (fig. 1(a) and (b)), but anisotropic in bcc metals because of the asymmetric geometry of TIS and OIS structure (fig. 1(c) and (d)).

The solution energies of He also can be deduced from the calculated stress tensor using the elastic theory [23], as listed in table 2. Relatively, He is predicted by the elastic stress model to favor the OIS in fcc metals, but the TIS in bcc metals, which is in good agreement with the DFT results. However, the absolute value of the individual solution energy as obtained from the stress model does not agree very well with the DFT calculated energy. One possible reason for this is that the elasticity

Table 2: Solution energy (in eV) of He given by the elastic calculations at the TIS over OIS in fcc and bcc metals.

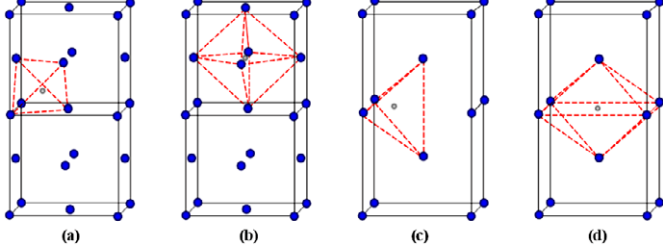|		fcc					bcc				
		Pd	Al	Au	Pt	Ag	W	Mo	Fe	Cr	V
Solution	TIS	0.23	0.33	0.67	0.57	0.33	0.10	0.09	0.22	0.16	0.11
energy	OIS	0.17	0.24	0.48	0.42	0.22	0.12	0.11	0.25	0.18	0.14

Fig. 1: (Colour on-line) The interstitial sites in fcc and bcc metals. (a) fcc, TIS; (b) fcc, OIS; (c) bcc, TIS; (d) bcc, OIS. The larger blue spheres represent the metal atoms, while the smaller gray spheres represent the He atoms.

Fig. 2: (Colour on-line) The ratio of solution energy vs. the ratio of He-induced stress at the TIS vs. OIS in fcc and bcc metals.

theory assumes a macroscopic continuum description, which cannot capture the detailed microscopic interaction between He and metal atoms, such as the displacement of metal atoms induced by He insertion. In addition, the lattice constant may change upon He doping, especially for a very large doping concentration we used in supercell DFT calculations. These and other factors make the direct comparison of absolute energies unfeasible.

Overall, however, the stress model prediction correlates closely with the solution energy: the OIS is favored in fcc metals but the TIS is favored in bcc metals. Most importantly, we plot in fig. 2, the relative stability of He at the TIS over the OIS as a function of the ratio of the He-doping induced elastic energy at the two sites, which agrees perfectly with eq. (1). Quantitatively, in fcc metals, the ratios are $E_s^{\mathrm{TIS}}/E_s^{\mathrm{OIS}} \sim 1.082$ and $\sum \sigma_{ii,\mathrm{TIS}}^2 / \sum \sigma_{ii,\mathrm{OIS}}^2 \sim 1.396$, giving rise to $\alpha_{\mathrm{fcc}} = 0.775$; in bcc metals, the ratios are $E_s^{\mathrm{TIS}}/E_s^{\mathrm{OIS}} \sim 0.954$ and $\sum \sigma_{ii,\mathrm{TIS}}^2 / \sum \sigma_{ii,\mathrm{OIS}}^2 \sim 0.856$, giving rise to $\alpha_{\mathrm{bcc}} = 1.114$. Thus, the He-induced lattice stress provides an accurate quantitative "indicator" of the effective volume of He in all the cases studied, providing an unambiguous way to assess the relative stability of He in different interstitial sites.

The embedding of He in metals is known to induce a volume change, i.e., formation volume, which has been used to characterize the doping stability. However, conventionally, formation volume is considered as a "scalar" indicating an "isotropic" uniform volume expansion/contraction. In contrast, the stress we introduce here is a "tensor" that can be anisotropic, as in the case for both TIS and OIS in bcc metals. An anisotropic stress means that the volume expansion/contraction is anisotropic, i.e. expansion/contraction is different
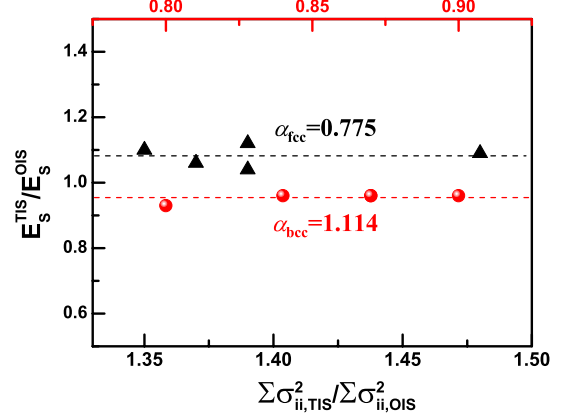
along different axes. This new insight is missing in the conventional picture of formation volume. Normally, one would calculate the formation volume by uniformly expand/shrink the lattice until the energy is minimized, which was in fact incorrect if the doping induced lattice stress is anisotropic. Instead, one should expand/shrink lattice by different amounts along different axes following the anisotropic stress values. Therefore, we have calculated the formation volume of He at the TIS and the OIS in metals by relaxing the lattice to minimize the stress tensor to zero, as listed in table 1. The resulting formation volume equals to the product of $\Delta V = \Delta a \times \Delta b \times \Delta c$, where $\Delta a, \Delta b$ and Δc scales with the stress values along the x-, y- and z-axis. Our calculated formation volume is shown in table 1 to characterize well the relative stability of He in metals. It is worthy to note that the stress model provides important new insight of the "shape" of formation volume given by stress anisotropy (ratios of σ_{ii}/σ_{jj}) in addition to the "size" of formation volume given by the trace of stress tensor ($\sum \sigma_{ii}$) [24]. Therefore, the stress approach should be preferred over the conventional volume approach because the stress, as a tensor, gives a more correct and complete picture than volume, as a scalar. As shown in table 1, the He-induced stress tensor is anisotropic for the asymmetry interstitial TIS and OIS sites in a bcc structure. This feature is not meant to be captured by a volume relaxation without the stress information. In some sense, the formation volume is an average effect of He induced stress, but it misses some microscopic details associated with the local

Table 3: Interstitial volume in units of a_0^3 based on different lattice models, where a_0 is the lattice constant.

Lattice model	$V_{\text{TIS}}^{\text{fcc}}$	$V_{\text{OIS}}^{\text{fcc}}$	$V_{\text{TIS}}^{\text{bcc}}$	$V_{\text{TIS}}^{\text{bcc}}$	$V_{\text{TIS}}^{\text{fcc}}/V_{\text{OIS}}^{\text{fcc}}$	$V_{\text{TIS}}^{\text{bcc}}/V_{\text{OIS}}^{\text{bcc}}$
Point-lattice	1/24	1/6	1/12	1/3	0.25	0.25
Voronoi	0.1319	0.1246	0.2568	0.2511	1.06	1.02
Hard-sphere	0.0021	0.0131	0.0084	0.0013	0.16	6.46

Table 4: The He-induced lattice strain estimated from different lattice models.

Lattice		fcc					bcc				
		Pd	Al	Au	Pt	Ag	W	Mo	Fe	Cr	V
Point-lattice	TIS	0.13	0.15	0.18	0.14	0.17	−0.08	−0.09	−0.22	−0.21	−0.15
	OIS	0.45	0.47	0.48	0.46	0.48	0.32	0.31	0.23	0.24	0.27
Voronoi	TIS	0.25	0.27	0.29	0.27	0.30	0.26	0.25	0.16	0.17	0.21
	OIS	0.24	0.26	0.28	0.24	0.29	0.25	0.25	0.16	0.16	0.20
Hard-sphere	TIS	−1.97	−1.89	−1.81	−1.94	−1.83	−1.32	−1.34	−1.61	−1.60	−1.48
	OIS	−0.61	−0.57	−0.53	−0.60	−0.54	−3.35	−3.42	−3.94	−3.88	−3.67

symmetry of interstitial site. Furthermore, the stress tensor is calculated only once at the equilibrium lattice constant without the need of lattice relaxation. This saves computational time than doing formation volume calculation which requires a number of lattice relaxation steps until the lowest-energy lattice is found.

Next, we examine which empirical lattice model is the most reasonable choice in estimating the effective volume of He, based on the quantitative stress indicators shown above. We consider three different lattice models: point-lattice, Voronoi polygon, and hard-sphere model, as shown in table 3. The point-lattice model was introduced as early as in the 17th century, which has been adopted most often in analyzing He interstitials in metals previously [5–7]. According to the point-lattice model, the TIS volume is four times smaller than the OIS volume in both fcc and bcc metals (table 3). Another popular ancient lattice model is the Voronoi polyhedron model originally introduced by Voronoi in 1907 [25]. According to the Voronoi model, the TIS volume is slightly larger than the OIS volume in both fcc and bcc metals (table 3), as calculated from a Voro++ code [26]. The third hard-sphere lattice model was originally introduced by Kepler in 1611 [27], as schematically depicted in fig. 3. According to the hard-sphere model, the TIS volume is much smaller than the OIS volume in fcc metals, while it is much larger than the OIS volume in bcc metals (table 3). Therefore, qualitatively, both the point-lattice and Voronoi models would predict the same behavior for He in fcc and bcc metals, contradicting with the first-principles results of He solution energies and stresses shown above; while only the hard-sphere model will predict a different behavior in the two types of metals, in agreement with the first-principles results. Despite such good agreement, the hard sphere model is a relatively simple model which can be
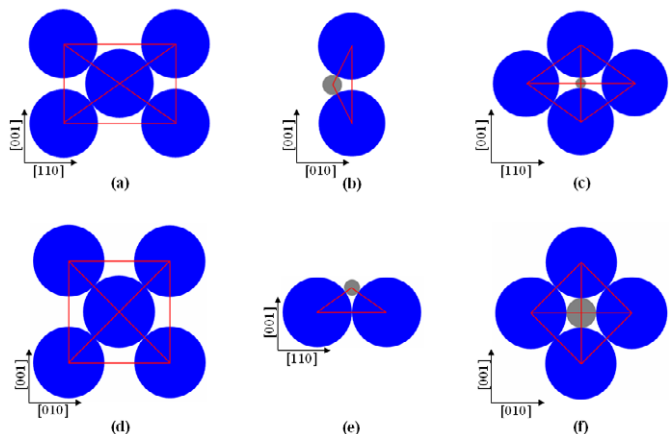

Fig. 3: (Colour on-line) Hard-sphere model for the TIS and OIS in bcc and fcc metals. (a) fcc, (100) plane; (b) fcc, TIS, (1 −10) plane; (c) fcc, OIS, (100) plane; (d) bcc, (1 −10) plane; (e) bcc, TIS, (100) plane; (f) bcc, OIS, (1 −10) plane. The larger blue spheres represent the metal atoms, while the smaller gray spheres represent the He atoms.

more conveniently used as an initial qualitative estimate without doing any calculation.

More specifically, one needs to compare the atomic volume of He with the available interstitial volume, as predicted from the different lattice models, to see how well the He atom fits in the lattice. We may estimate the He-induced lattice stress or strain (ε) occupying an interstitial site in metals by

$$\varepsilon = -\frac{R_{\text{He}} - R_{\text{int}}}{R_{\text{int}}}, \qquad (2)$$

where $R_{\text{He}} = 0.93\,\text{Å}$ is the covalent radius of He [28], and R_{int} is the effective radius of interstitial sites. In eq. (2) we

use the sign convention so that if R_{He} is larger (smaller) than R_{int}, the He atom induces a "negative" compressive ("positive" tensile) lattice strain. We calculate R_{int} using different lattice models by approximating the interstitial volume (see table 3) as a sphere. Table 4 shows only the hard-sphere model gives the compressive strains for He in both fcc and bcc metals, consistent with the first-principles stress results (table 1). It indicates that the atomic volume of He is larger than the effective volume of interstitial sites in all the cases. In contrast, the point-lattice and Voronoi models give the wrong sign of strain or the size of effective volume, except the case of bcc TIS by the point-lattice model. This shows that only the hard-sphere model is qualitatively correct to be used as an empirical "indicator" to assess the effective interstitial volume for He in metals. Quantitatively, however, the model overestimates the difference between the TIS and OIS.

We believe that the quantitative stress "indicator" will be applicable not only to interstitial sites, but more generally also to other cases including defects such as vacancy, dislocation or grain boundary in metals. For example, our calculations show that He at a monovacancy site in bcc W induces an isotropic compressive stress of $-0.33\,\mathrm{GPa}$, given the symmetric local geometry. It is much lower than the compressive stress induced by the He at the TIS and OIS in W (see table 1). This suggests the effective volume of He is largest at the monovacancy. The relative stability of He is found in descending order from vacancy to TIS and to OIS from both stress model and direct DFT solution energies.

In conclusion, we demonstrate a theoretical scheme to quantify the effective volume and hence stability of He in metals. We show that the effective volume can be approximated by the hard-sphere lattice model, but not the point-lattice or the Voronoi polygon model. We propose that the effective volume and thus the relative stability of He at different interstitial sites can be quantitatively characterized by the He-induced lattice stresses in metals. We believe that the concept of stress indicator is generally applicable to quantify the relative stability of other inert gas elements in metals.

$$* * *$$

REFERENCES

[1] Barnes R. S., *Nature*, **206** (1965) 1307.
[2] Ullmaier H., *Nucl. Fusion*, **24** (1984) 1039.
[3] Bloom E. E., *J. Nucl. Mater.*, **258** (1998) 7.
[4] Maloy S. A., James M. R., Johnson W. R., Byun T. S., Farrell K. and Toloczko M. B., *J. Nucl. Mater.*, **318** (2003) 283.
[5] Seletskaia T., Setsky Y., Stoller R. E. and Stocks G. M., *Phys. Rev. Lett.*, **94** (2005) 046403.
[6] Seletskaia T., Osetsky Y., Stoller R. E. and Stocks G. M., *Phys. Rev. B*, **78** (2008) 134103.
[7] Zu X. T., Yang L., Gao F., Peng S. M., Heinisch H. L., Long X. G. and Kurtz R. J., *Phys. Rev. B*, **80** (2009) 054104.
[8] Yang L., Zu X. T. and Gao F., *Physica B*, **403** (2008) 2719.
[9] Zeng X. L., Deng H. Q. and Hu W. Y., *Nucl. Instrum. Methods Phys. Res. B*, **267** (2009) 3037.
[10] Fu C.-C. and Willaime F., *Phys. Rev. B*, **72** (2005) 064117.
[11] Becquart C. S. and Domain C., *Phys. Rev. Lett.*, **97** (2006) 196402.
[12] Kresse G. and Hafner J., *Phys. Rev. B*, **47** (1993) 558.
[13] Kresse G. and Furthmüller J., *Phys. Rev. B*, **54** (1996) 11169.
[14] Perdew J. P. and Wang Y., *Phys. Rev. B*, **45** (1992) 13244.
[15] Blöchl P. E., *Phys. Rev. B*, **50** (1994) 17953.
[16] Jiang D. E. and Carter E. A., *Acta Mater.*, **52** (2004) 4801.
[17] Yuan D. W., Gong X. G. and Wu R. Q., *Phys. Rev. B*, **75** (2007) 085428.
[18] Tung J. C. and Guo G. Y., *Phys. Rev. B*, **81** (2010) 094422.
[19] Liu M., Qin X., Liu C. S., Pan L. and Xin H. X., *Phys. Rev. B*, **81** (2010) 245215.
[20] Razumovskiy V. I., Ruban A. V. and Korzhavyi P. A., *Phys. Rev. B*, **84** (2011) 024106.
[21] Monkhorst H. J. and Pack J. D., *Phys. Rev. B*, **13** (1976) 5188.
[22] Huang B., Liu M., Su N. H., Wu J., Duan W. H., Gu B. L. and Liu F., *Phys. Rev. Lett.*, **102** (2009) 166404.
[23] Clouet E., Garruchet S., Nguyen H., Perez M. and Becquart C. S., *Acta Mater.*, **56** (2008) 3450.
[24] Landau L. D. and Lifshitz E. M., *Theory of Elasticity, Course of Theoretical Physics*, Vol. **7** (Pergamon Press, London) 1959.
[25] Voronoi G., *Reine Angew. Math.*, **133** (1907) 97.
[26] Rycroft C. H., Grest G. S., Landry J. W. and Bazant M. Z., *Phys. Rev. E*, **74** (2006) 021306.
[27] Torquato S. and Stillinger F. H., *Rev. Mod. Phys.*, **82** (2010) 2633.
[28] Ahrens L. H., *Geochim. Cosmochim. Acta*, **2** (1952) 155.